

## SINGLE-ENDED FAULT LOCATION TECHNIQUE ON A RADIAL DISTRIBUTION NETWORK USING FAULT GENERATED CURRENT SIGNALS

H. Hizam<sup>1</sup> and P. A. Crossley<sup>2</sup>

<sup>1</sup>Department of Electrical and Electronic Engineering, Universiti Putra Malaysia, 43400 Selangor, Malaysia

<sup>2</sup>School of Electrical and Electronic Engineering, Queen's University of Belfast, UK

Email: [hashim@eng.upm.edu.my](mailto:hashim@eng.upm.edu.my)

### **ABSTRACT**

*High frequency signals generated due to faults contain information which could be utilised to locate the faults. Based on the principle of reverberation of waves on power network, the high frequency signature of the current signals are related to known reflection points exist in the network. From these the fault section and the probable location of the fault can be identified. The probable location is then used within a power system simulator that models the network. The simulated current waveforms at the probable locations are then cross-correlated against the signals captured. If the identified location is correct, the high frequency signature in the simulated waveform will be similar to that observed in the measured waveform and the cross-correlation value will have a high positive value. If the signatures differ, the cross-correlation value will be small. Simulation studies using PSCAD/EMTDC and analysis using cross-correlation indicate that locating faults on a radial distribution feeder is a possibility using a single ended travelling wave measurement method.*

**Keywords:** *fault location, travelling waves, distribution network, cross-correlation*

### **INTRODUCTION**

Power systems are regularly subjected to unexpected disturbances, which occasionally result in the occurrence of short circuit faults. When a fault occurs, the current and voltage become abnormal and consequently the result is an unsatisfactory delivery of power to the consumers. Since faults can destabilise the power system, they must be isolated quickly. Finding the accurate location of a fault has always been a challenge for electric utilities.

Conventional method of fault location is to use the voltage and current data measured at one or more points along the power networks. Knowing the line impedance per unit length, the fault distance can be approximated from the calculated impedance obtained from the voltage and current data. This impedance method, however, is subject to errors caused by for example high resistance ground faults, teed circuits topologies, and the interconnection to multiple sources [1].

The other technique used is the travelling waves method [2-10]. In all these techniques, the high frequency transients are used instead of the steady state components to determine the location of the fault. Single-ended and double-ended techniques have been used to determine the fault location using travelling waves [11]. For single-ended, the current or voltage signals are measured at one end of the line and fault location relies on the analysis of these signals to detect the reflections that occur between the measuring point and the fault. For the double-ended method, the time of arrival of the first fault generated signals are measured at both ends of the lines using synchronised timers. The double-ended method does not require multiple reflections of the signals. However, single-ended location is preferred as it only requires one unit per line and a communication link is not necessary [6]. Therefore for distribution systems, it should be less expensive and consequently preferable.

### **BASIC PRINCIPLES OF TRAVELLING WAVES FAULT LOCATION**

The basic principle of most single-ended travelling wave fault locators is to evaluate the fault location using the time difference between the first arrival of an incident travelling wave generated by a fault and the corresponding reflected wave reflected from the fault point [2,4]. However, since travelling waves are reflected by other discontinuities, identification of the desired signal is of crucial importance to the accuracy of the fault location [4]. The most widely used analysis method is based on cross-correlation; the incident travelling wave is taken as a reference and the signal that contains the subsequent backward travelling waves is cross-correlated

with the reference. The basic principle is that the desired backward travelling waves would have the same shape as the reference and would generate a peak in the correlation output.

Existing travelling wave based fault locators have been applied to transmission lines rather than distribution lines. This is because distribution lines are comparatively short in length and consequently it is difficult to detect separately the arrival of a fault generated incident wave and the arrivals of the subsequent backward travelling waves [12]. Furthermore, a distribution line usually contains many branches, which would produce multiple reflections and reduce the magnitude of the travelling waves as they propagate along the line. These branches complicate the process of identifying the desired signal. The basic principle of a travelling wave based fault locator can be described by considering Figure 1.

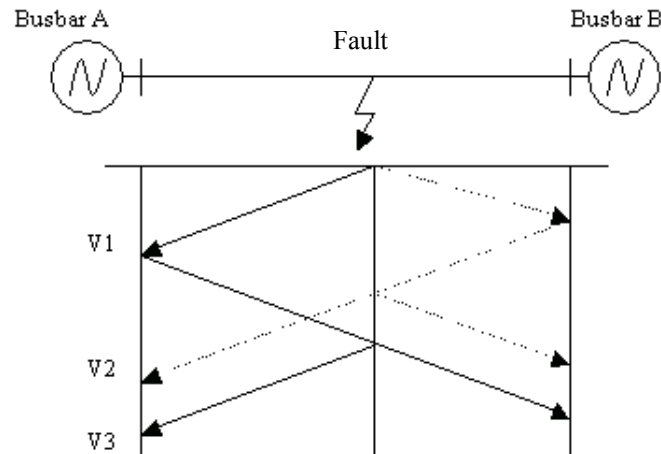


Figure 1: Bewley Lattice diagram

When a fault occurs on power lines, voltage and current travelling waves will be generated which propagate away from the fault in opposite directions towards the busbars. As these waves reach the busbars (assuming total reflection factor at the busbars), they are reflected back towards the fault point. As they arrive at the fault point, a part of the wave will be re-reflected back towards one end and a part will be transmitted through to the other end. This process continues until the signals die out due to attenuation. The voltage and current generated travelling waves can be expressed in term of a forward,  $f_1$ , and a backward,  $f_2$ , travelling waves by [6]:

$$v(x, t) = f_1(t - x/c) + f_2(t + x/c) \quad (1)$$

$$i(x, t) = \frac{1}{Z_0} f_1(t - x/c) - \frac{1}{Z_0} f_2(t + x/c) \quad (2)$$

where  $c$  is the velocity of wave propagation,  $Z_0$  is the characteristic impedance of the lines, and  $x$  is the distance that the waves travel away from the fault point. The forward,  $f_1$ , and backward,  $f_2$ , travelling waves, on the other hand, can be written as:

$$f_1 = v(x, t) + Z_0 i(x, t) \quad (3)$$

$$f_2 = v(x, t) - Z_0 i(x, t) \quad (4)$$

Referring to Figure 1 and assuming that measurements are taken at busbar A, if the time interval between the arrival of the forward wave V1 and that of the backward wave V3 is obtained, the distance to the fault from busbar A can be calculated as follow:

$$d = ct/2 \quad (5)$$

where  $c$  is the travelling wave velocity and  $t$  is the time interval.

## THE FAULT LOCATION ESTIMATION METHOD

In a fault locator based on high frequency travelling waves, the time delay between the arrival of the fault injected signal and the appropriate reflected signal is measured. This can be implemented relatively simply. The complexity occurs in identifying the reflected signal that has travelled from the monitoring location to the fault and back. A method that can be used to detect the desired surge is based on an auto-correlation technique. Auto-correlation determines the similarity between events within a signal and can be used to detect when the reflected signal appears in the captured waveform [13]. To implement this technique, a section of the captured signal is stored and used as a reference. It is then auto-correlated with the rest of the signal. The next peak in the auto-correlation function suggests that the delayed section of the signal closely matches the reference signal. This time delay can then be used to calculate the distance to the fault. This method works well on a simple two terminal transmission line but for a more complicated network that consists of several branches, this auto-correlation technique might not be able to detect the desired signal correctly.

This paper proposes a simple technique that compares the relative distance of each “peak” in the high frequency signal with the known reflection points in the network. From these the fault section and the probable location of the fault can be identified. The probable location is then used within a transient power system simulator (PSCAD/EMTDC) that models the actual distribution feeder and all its spurs. The simulated current waveforms are then cross-correlated against the original signal. If the identified “probable” location is correct, the high frequency signature in the simulated waveform will be similar to that observed in the measured waveform and the cross-correlation value will have a high positive value. If the signatures differ, the cross-correlation value will be small or negative and the process must be repeated using the next most likely fault location.

## POWER SYSTEM MODELLING

An 11 kV distribution feeder was modelled using PSCAD/EMTDC [14]. The one line diagram of the distribution feeder is shown in Figure 2.

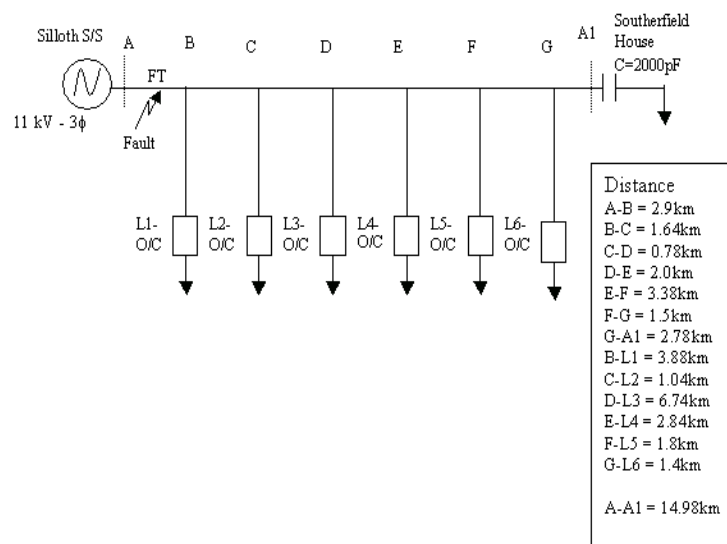


Figure 2: One line diagram

For the initial study, the network was assumed to be entirely overhead and the conductor parameters are chosen as follows:

- Number of conductors : 3
- Conductor radius: 0.005025 m
- Conductor DC resistance: 0.5426 ohm/km
- Height of conductors above the ground: 6 m

- Horizontal spacing between phases: 0.8 m
- Ground wires: none
- Ground resistivity: 100 ohm.m

The characteristic impedance of the line is  $348\Omega$  and the velocity of the travelling wave is almost  $3 \times 10^5$  km/s, i.e. the speed of light.

A Phase A to earth fault was simulated at various points along the main feeder with current measurement taken at point A. The fault resistance for this study was chosen as  $0.01\Omega$  and the time step for the simulation was  $0.8 \mu\text{s}$ . The measurement was taken at point A of Figure 2.

## RESULTS AND DISCUSSIONS

Figure 3 shows the current waveforms when a Phase A to earth fault was simulated at a distance 2 km from the measurement point A (the fault is between measurement point A and the first branch, B).

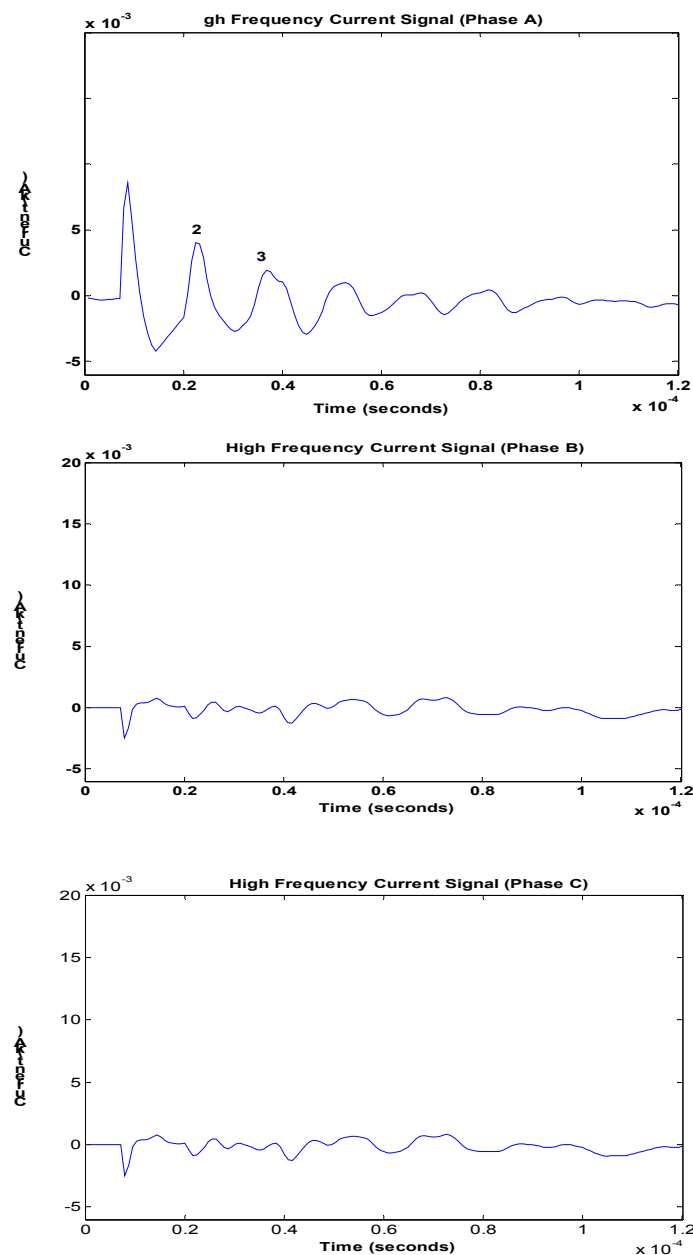


Figure 3: Current waveforms for Phase A, B and C for a fault at a distance of 2 km

Comparing the magnitudes of all three phase currents reveals that the magnitude of the phase A current is significantly larger. Therefore it is concluded that the fault is a phase A to earth. Having determined the type of fault, the fault location is evaluated using the faulted phase waveform. The phase A current signal shows that the highest peak occurs immediately after the occurrence of the fault. The time delay between this peak (1) and the time that the fault occurred is  $8\mu\text{s}$ . If this time difference is multiplied by the velocity of the travelling wave ( $3 \times 10^5 \text{ km/s}$ ), the distance from point A is 2.4 km. This first peak is as expected the first incident travelling wave, i.e. the wave initiated by the fault. The second peak, (2), occurs after a time delay of  $21.6\mu\text{s}$ , which corresponds to a total distance travelled of 6.48 km. The second peak is apparently the reflected wave from the fault point as the distance travelled is about three times the distance from the fault point to point A. In practice, the exact time at which the fault occurs is not known and therefore the first incident surge (peak 1) is used as a reference and the time difference between the first surge and subsequent surges is used to determine the corresponding distances. Table 1 tabulates the time delay of the peaks with respect to peak 1. Equation (5) is used to calculate the half distance travelled by a surge that leaves the monitoring point at peak 1 and returns at peak 2,3...etc.

Table 1: Calculated distance of each peak relative to peak 1 for a fault at 2 km

Peak	Time Delay ( $\mu\text{seconds}$ )	Distance (km)
1	0.0	0.00
2	13.6	2.04
3	27.2	4.08

Since the fault occurs at a point where there is no branch in between point A and B the fault surge will travel back and forth between these two points and therefore peak 2 can be easily identified as the surge reflected from the fault point. Peak 3 has a corresponding distance of twice the distance from the fault point to point A and is the surge reflected from the fault point for the second time.

For a fault distance of 3.9 km, i.e. a location between B and C, the faulted phase current waveform is as shown in Figure 4.

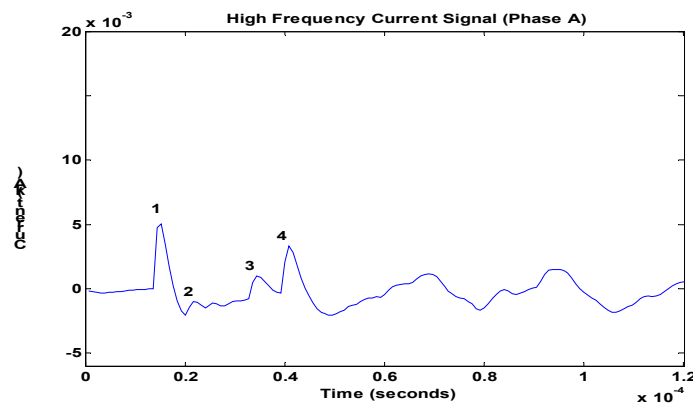


Figure 4: Phase A current waveform for a fault at a distance of 3.9 km

With reference to the phase A current waveform, the time delay of each current peak with respect to peak 1 and the corresponding distances are shown in Table 2.

Table 2: Calculated distance of each peak relative to peak 1 for a fault at 3.9 km

Peak	Time Delay ( $\mu\text{seconds}$ )	Distance (km)
1	0.0	0.0
2	7.2	1.08
3	19.2	2.88

4	27.2	4.08
---	------	------

The existence of a branch between the fault point and the measurement point A produces multiple reflection signals and it is more difficult to interpret the waveform. Analysis based on the distance calculated relative to the incident surge suggests that peak 3 is the surge reflected from the first T point (B). This interpretation is made because the distance from point A to point B is close to the distance corresponding to peak 3. Peak 2 cannot be the surge reflected from the fault point, as the distance corresponding to this peak would mean that the fault is between point A and B. As shown in the case of a fault at a distance of 2 km, the fault between these two points would produce a more defined waveform, as the surge would then only reverberate between the two points. In this case peak 2 actually corresponds to a surge that travels in the path FT-B-FT-B-A. Peak 4 is the surge that is reflected from the fault point. This is the surge that gives the correct distance to the fault.

For a fault distance of 4.94 km, i.e. a location between C and D, the phase A current waveform is as shown in Figure 5.

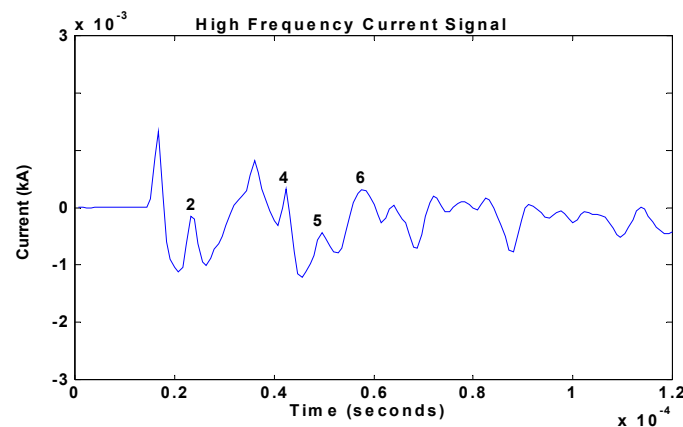


Figure 5: Phase A current waveform for a fault at a distance of 4.94 km

With reference to the phase A current waveform, the time delay of each current peak and the corresponding distances with respect to peak 1 are shown in Table 3.

Table 3: Calculated distance of each peak relative to peak 1 for a fault at 4.94 km

Peak	Time Delay ( $\mu$ seconds)	Distance (km)
1	0.0	0.00
2	7.2	1.08
3	19.2	2.88
4	25.6	3.84
5	32.8	4.92
6	41.6	6.24

Comparing the calculated distances to the known distances, the following conclusions can be made:

1. Peak 2 corresponds to the surge travelling the path FT-C-L2-C-B-A. This conclusion was made because peak 1 corresponds to the path FT-C-B-A and the additional distance in travelling down branch C-L2 is 1.04 km.
2. Peak 3 corresponds to the surge that is reflected from the first T point (point B) –i.e. path FT-C-B-A-B-A; for this peak the calculated distance is close to the distance from point A to B (2.9 km).
3. Peak 4 corresponds to the surge travelling the path FT-C-B-L1-B-A; for this peak the calculated distance is close to the length of branch B-L1 (3.88 km).
4. Peak 5 whose distance relative to peak 1 is 4.92 km does not correspond to any known distance in the network and this peak might be the surge reflected from the fault point. This can be confirmed by

simulating the fault at this location and cross correlating the simulated waveform with the original waveform. A large correlation coefficient indicates a high degree of similarity between the shapes of the two waveforms. Since there are reflection signals from branch B-L1 and branch C-L2, it can be concluded that the faulty section would be between point C and D.

As the fault location moved away from the source, the current waveforms become more and more complex. This is because of multiple reflections from the T points and ends of each branch. This is illustrated by considering the current waveforms in Figures 3, 4, and 5. For Figure 5, the waveform was obtained when the fault was at a location where two branches are between the fault and the measurement point. To observe the effect on its current waveforms of moving the fault further away, a fault at 9.32 km (between E and F) was simulated. The resulting current waveform is shown in Figure 6.

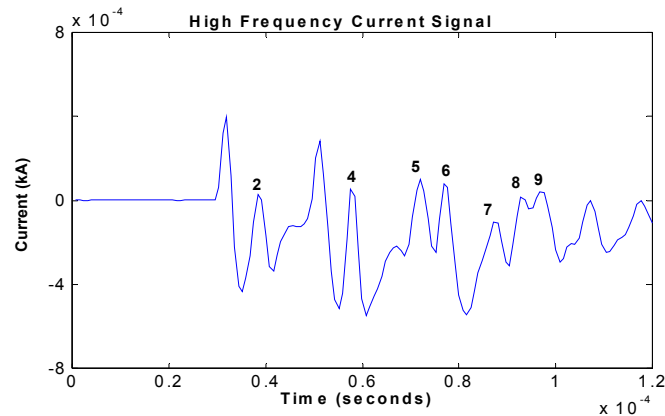


Figure 6 : Phase A current waveform for a fault at a distance of 9.32 km

The time delay of each peak with respect to peak 1 and the corresponding distances are shown in Table 4.

Table 4: Calculated distance of each peak relative to peak 1 for a fault at 9.32 km

Peak	Time Delay ( $\mu$ seconds)	Distance (km)
1	0.0	0.00
2	6.4	0.96
3	19.2	2.88
4	24.8	3.72
5	40.0	6.00
6	44.8	6.72
7	55.2	8.28
8	60.8	9.12
9	65.6	9.84

The existence of several branches between the fault and the measurement point makes it more difficult to trace the path of the surge corresponding to a peak. However, there are some peaks whose corresponding distances relative to peak 1 are close to some of the known distances. For example:

1. Peak 2 corresponds to a distance of 0.96 km, which is close to a known distance of branch C-L2 (1.04 km).
2. Peak 3 corresponds to a distance of 2.88 km. This can be assumed to be a surge reflected from either point B (the distance from A to B is 2.9 km) or point L4 (the length of branch E-L4 is 2.84 km) or a combination of both.
3. Peak 4 is the surge reflected from point L1 as the calculated distance is close to the length of branch B-L1 (3.88 km).
4. Peak 6 is the surge reflected from L3 as the calculated distance is close to the length of branch D-L3 (6.74 km).

The other calculated distances cannot be easily related to any of the known distances in the network. From the conclusions, the faulty section can be identified as between point E and F since there are reflection signals from branch B-L1, C-L2, D-L3 and E-L4. Knowing the faulty section, the distance to the fault can be estimated to be between 7.32 km and 10.70 km.

**CROSS-CORRELATION ANALYSIS**

From the relative distances calculated in section 4.1, faults can be simulated at the probable locations. The simulated current waveforms can then be compared with the original waveforms. Table 5 summarises the most probable fault locations for each case.

*Table 5: Probable fault locations*

Actual Fault Distance (km)	Probable Fault Distances (km)
2.0	2.04
3.9	4.08
4.94	4.92
9.32	8.28, 9.12, 9.84

The waveform comparison between the original signals and the signals at the probable fault locations are shown in Figure 7a, 7b, 8a, 8b, 9a, 9b, 10a, 10b, 10c, and 10d.

**Case 1: Fault distance at 2.0 km**

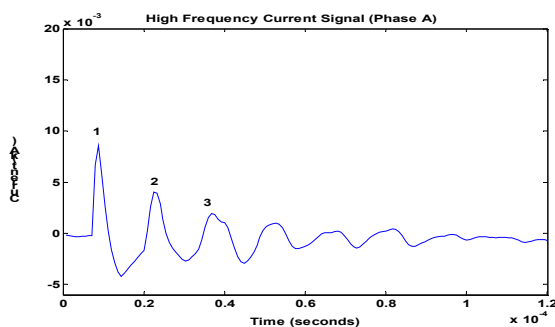


*Figure 7a: Original signal for a fault at 2 km*

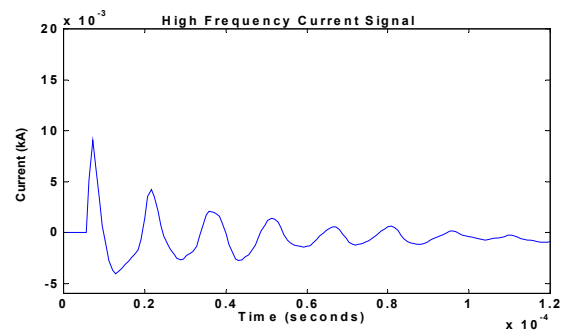


*Figure 7b: Simulated signal for a fault at 2.04 km*

A visual inspection of Figures 7a and 7b indicates that the signals are very similar hence the fault must be approximately 2 km from Silloth on section A-B.

**Case 2: Fault distance at 3.9 km**

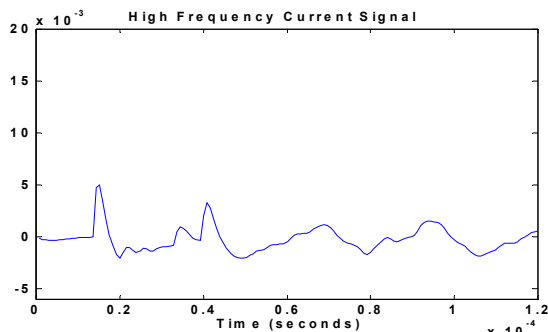


*Figure 8a: Original signal for a fault at 3.9 km*

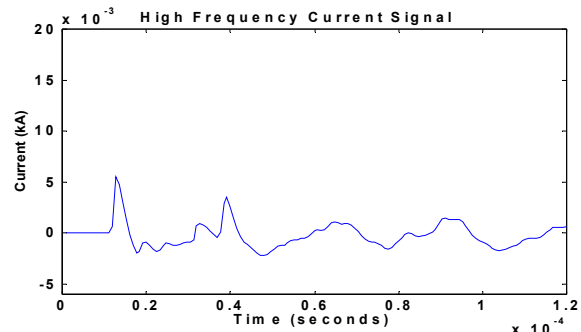


*Figure 8b: Simulated signal for a fault at 4.08 km*

Similarly, Figures 8a and 8b are very similar; hence the fault must be approximately 4 km from Silloth on section B-C.

**Case 3: Fault distance at 4.94 km**

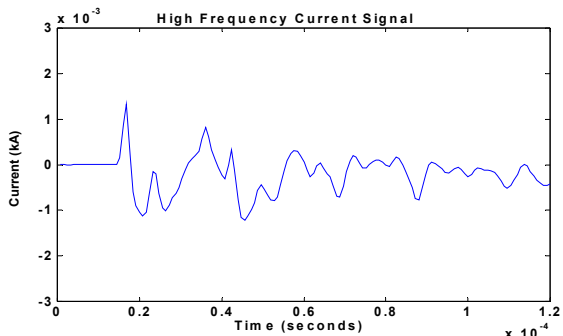


Figure 9a: Original signal for a fault at 4.94 km

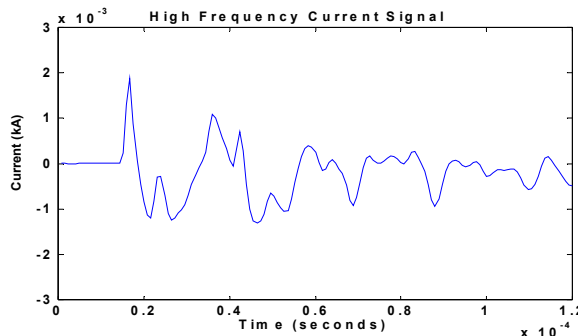


Figure 9b: Simulated signal for a fault at 4.92 km

A visual inspection of Figures 9a and 9b indicates that the signals are very similar; hence the fault must be approximately 5 km from Silloth on section C-D.

**Case 4: Fault distance at 9.32 km**

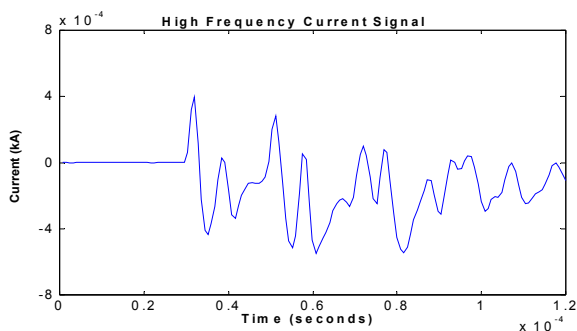


Figure 10a: Original signal for a fault at 9.32 km

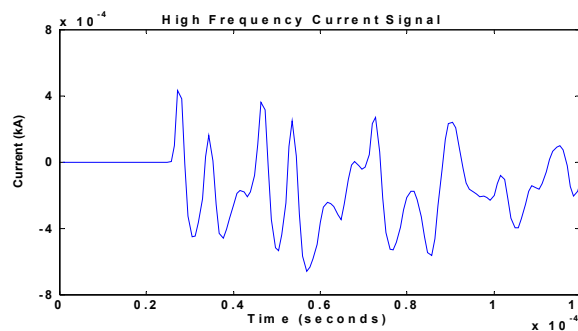


Figure 10b: Simulated signal for a fault at 8.28 km

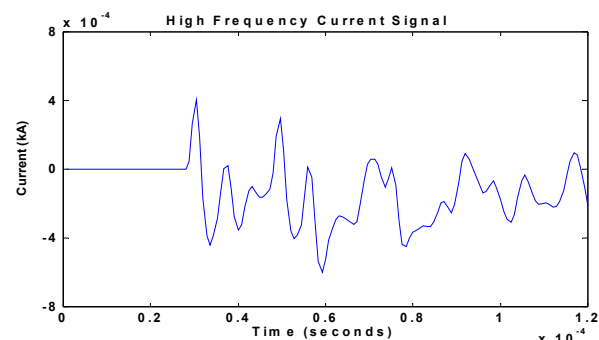


Figure 10c: Simulated signal for a fault at 9.12 km

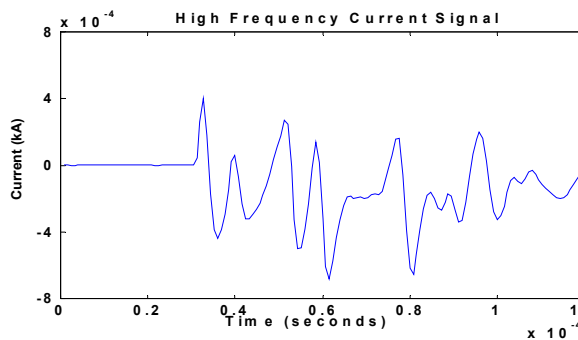


Figure 10d: Simulated signal for a fault at 9.84 km

A visual inspection of the signal shown in Figure 10 indicates that the waveform of Figure 10c is the one that closest matches the original signal (Figure 10a).

In order to determine the degree of similarity between the original signals and the signals simulated at the probable fault locations, a technique based on cross-correlation was used. The correlation coefficients for each fault distance are summarised in Table 6, 7, 8 and 9.

Table 6: Correlation coefficient for probable fault distances for a fault at 2.0 km

distance (km)	Cross-Correlation Window			Average
	Correlation Coefficient (CC)			
2.04	50	75	100	0.9794
	0.9847	0.9786	0.9749	

Table 7: Correlation coefficient for probable fault distances for a fault at 3.9 km

distance (km)	Cross-Correlation Window			Average
	Correlation Coefficient (CC)			
4.08	50	75	100	0.9745
	0.9744	0.9757	0.9735	

Table 8: Correlation coefficient for probable fault distances for a fault at 4.94 km

distance (km)	Cross-Correlation Window			Average
	Correlation Coefficient (CC)			
4.92	50	75	100	0.9367
	0.9376	0.9351	0.9373	

Table 9: Correlation coefficient for probable fault distances for a fault at 9.32 km

distance (km)	Cross-Correlation Window			Average
	Correlation Coefficient (CC)			
8.28	50	75	100	0.8836
	0.9318	0.8670	0.8519	
9.12	50	75	100	0.9434
	0.9751	0.9370	0.9181	
9.84	50	75	100	0.8530
	0.9222	0.8294	0.8075	

The above results indicate that the maximum correlation coefficients are obtained for peaks whose corresponding distances are closest to the actual fault distances. The errors range from 20 to 200 meters.

## CONCLUSIONS

This study suggests that by calculating the relative distance of the “peak” in the high frequency travelling waves and comparing it with the known distances in the distribution feeder, it is possible to identify the faulty section and the probable location of the fault. From the simulation results the fault locations can be estimated with accuracies of 200 meters. This technique is especially attractive because the location can be estimated using only one measurement point, thus eliminating the need for communication link between two or more measuring points and is more economical.

## REFERENCES

- [1] Crossley PA, Gale PF, Bingyin Xu, Yaozhong Ge, Cory B.J, Barker JRG. (1993) Fault location based on travelling waves. Fifth International Conference on Developments in Power System Protection, Conference Publication No. 368, 54-59.
- [2] Crossley P.A. & MacLaren P.G. (1983) Distance protection based on travelling waves. IEEE Transactions on Power Apparatus and System **102** (9): 2971-2983.
- [3] Ancell G.B. & Pahalawaththa N.C. (1994). Maximum likelihood estimation of fault location on transmission lines using travelling waves. IEEE Transactions on Power Delivery **9**(2): 680-689.
- [4] Jie Liang, Elangovan S., Devotta J.B.X. (1999) Adaptive travelling wave protection algorithm using two correlation functions. IEEE Transactions on Power Delivery, **14**(1): 126-131.
- [5] Bo Z.Q., Weller G., Redfern M.A. (1999) Accurate fault location technique for distribution system using fault-generated high-frequency transient voltage signals. IEE Proceedings - Generation, Transmission and Distribution **146**(1): 73 – 79.
- [6] Crossley P.A., Gale P.F, Aurangzeb M. (2001) Fault location using high frequency travelling waves measured at a single location on a transmission line. Developments in Power System Protection, Amsterdam, Holland, 9-12 April, 403-406.
- [7] Elhaffar, A., Lehtonen, M. (2004) Travelling waves based earth fault location in 400 kV transmission network using single end measurement. Large Engineering systems Conference on Power Engineering, LESCOPE-04, 28-30 July, 53 – 56.
- [8] Thomas, D.W.P., Christopoulos, C., Tang, Y., Gale, P., Stokoe, J. (2004) Single ended travelling wave fault location scheme based on wavelet analysis. Eighth IEE International Conference on Developments in Power System Protection, Volume 1, 5-8 April, 196 – 199.
- [9] Zeng Xiangjun, Li, K.K., Liu Zhengyi, Yin Xianggen (2004) Fault location using traveling wave for power networks. Industry Applications Conference, 2004, 39th IAS Annual Meeting, 3-7 October, 2426 – 2429.
- [10] Evrenosoglu, C.Y., Abur, A. (2005) Travelling wave based fault location for teed circuits. IEEE Transactions on Power Delivery **20**(2):1115 – 1121.
- [11] Gale P.F. and Giannattasio B.F. (1994) Travelling waves get to the point. Modern Power Systems :45-47.
- [12] [6] Bo Z.Q., Johns A.T. and Aggarwal R.K. (1997) A very accurate fault location technique for distribution line with tapped-off load. Proceedings of the 32<sup>nd</sup> UPEC conference, Vol. 1, 432-435.
- [13] Carl W. Helstrom (1984) *Probability and Stochastic Processes for Engineers*. MacMillan Publishing Company, New York.
- [14] (2000). *PSCAD/EMTDC Version 3 Getting Started Manual*, Manitoba HVDC Research Centre Inc., Canada.